Fibers and Polymers 2022, Vol.23, No.5, 1171-1181
DOI 10.1007/s12221-022-4001-y

ISSN 1229-9197 (print version)
ISSN 1875-0052 (electronic version)

Lead Removal from Aqueous Solution by Green Solid Film Based on Cellulosic Fiber Extracted from Banana Tree Doped in Polyacrylamide

Amr Abdelkhalek[1,2], Safaa S. M. Ali[3], Zhanwu Sheng[2]*, Lili Zheng[2], and Mohamed Hasanin[4]*

[1]*Horticultural Crops Technology Department, National Research Centre, Cairo 12622, Egypt*
[2]*Hainan Key Laboratory of Banana Genetic Improvement, Haikou Experimental Station, Chinese Academy of Tropical Agricultural Sciences, Haikou 571101, China*
[3]*Spectroscopy Department, Physics Division, National Research Centre, Cairo 12622, Egypt*
[4]*Cellulose and Paper Department, National Research Centre, Dokki, Cairo 12622, Egypt*
(Received January 4, 2021; Revised July 29, 2021; Accepted September 9, 2021)

Abstract: In the present study, we investigated the lead ions removal on the solid form (as strips) by adsorption on green cellulosic fiber/polyacrylamide (GCFP). Strips were prepared in a solid form, not a hydrogel, for performing the adsorption process without squandering of water. Then, the prepared film and its original materials were characterized using attenuated total reflection infrared spectroscopy (ATR-FTIR), and scanning electron microscopy with energy dispersive electron spectroscopy (SEM-EDX). The experiments were conducted under different operating conditions, such as contact time, initial Pb concentration, adsorbent dose, and pH value. The adsorption process mechanism was tested by applying two kinetic models to the experimental data, which are the pseudo-first order and the pseudo-second order, and intraparticle diffusion models. The equilibrium results were fitted to three isotherm models, namely Langmuir, Freundlich, and Dubinin-Radushkevich (D-R) models. We found a Pb removal yield of 98 % (approximately 128 mg/g) at pH=7, an adsorbent dose of 0.4 g, an initial Pb concentration of 50 ppm, and a contact time of 60 min. The kinetic study results showed that the pseudo-second-order kinetic model provided superior correlation for the adsorption of Pb ions. Moreover, Dubinin-Radushkevich isotherm model had better-fit adsorption data. The obtained results revealed the high efficiency of GCFP films in lead ions adsorption from water. Additionally, the components of these films, represented here by banana pseudo-stem waste, are green sources, inexpensive and easy to obtain, whereas this waste is a burden on the farmers due to its difficult disposal.

Keywords: Lignocellulose, Lead, Waste water, Banana fibers, Adsorption isotherms and kinetics

Introduction

Heavy metals removal from wastewater is an effective method for detoxification [1]. Adsorption is an important mechanism employed for wastewater treatment as it provides higher efficiency and easier material recyclability at a lower price [2] than other methods, such as flocculation/coagulation [3], membrane separation [4], chemical precipitation [5], oxidation [6], and electrochemical processes [7]. Toxic metal pollutants are widespread in industrial wastewater (i.e., in battery, electroplate, dye, and pigment production) [8-11]. Heavy metals are generally referred to as metals which possess a specific density of more than 5 g/cm^3 and negatively affect the environment and living organisms [12,13]. Heavy metals are considered to be environmentally significant pollutants, and their toxicity is of crucial importance in environmental, evolutionary, nutritional, and ecological aspects [13,14]. Wastewater contains abundant heavy metals, the predominant of which are arsenic, cadmium, chromium, copper, lead, nickel, and zinc, all of which pose risks to human health and the environment [15,16]. Heavy metals enter the environs through natural sources and human activities [17]. These metals are bound to protein sites in the cell of living organisms, displacing the original metal component from their natural binding sites and causing cell dysfunction that is manifested as toxicity [18]. Previous research has shown that oxidative decay of biological macromolecules is mostly due to the binding of heavy metals to DNA and nuclear proteins [19]. Lead, one of the most prevalent heavy metals in soil, is among the most toxic to humans, animals, and plants even in very low concentration. It has no known biological purpose but can cause morphological, physiological, and biochemical disorders in plants [20]. Lead is transferred from the soil to all plant parts through absorption by the root system, which poses an imminent threat to human health when edible plant parts are consumed; hence, water and soil contamination with lead poses doubled risks to humans, especially to children and women, as well as to crop production itself [21]. Lead is the most toxic heavy metal to the human organism, with an adverse influence on a considerable number of cell functions. Lead poisoning is manifested by many symptoms, but one of the most severe is the anemia it causes through the inhibition of porphobilinogen synthase and ferrochelatase, which blocks heme synthesis [22]. In addition, it causes serious disruption of human organ functions. For example, lead poisoning suppressed the respiratory functions of lead-exposed workers, in whose blood samples, high levels of the heavy metal were also detected [23].

*Corresponding author: shengzhanwu100@163.com
*Corresponding author: sido_sci@yahoo.com

Agricultural biowaste is considered a huge pollutant based on the by-product amounts produced, considered zero-value waste [24-29]. Moreover, biomass accumulation in the environment may lead to many hazards [29-31]. Banana fibers are widely available globally as agricultural waste from banana cultivation. The decomposition of the residues left on field results in the emission of huge amounts of carbon dioxide and methane gases. These emissions have a negative impact on the environment, constantly increasing the global warming effect [32]. On the other hand, banana fibers are environmentally friendly and have some important attributes, such as low density, light weight, and low cost. This waste, consisting of leaves, stems, and rhizomes, which is left in the field for natural degradation for months after fruit harvesting can be utilized in different applications, such as cellulose production and heavy metals adsorption from water [33,34]. Banana pseudo-stem consists mainly of cellulose, which can be used as an adsorbent for heavy metals after chemical grafting. Therefore, this work is aiming at assessing the heavy metal adsorption potential of this biomaterial. We employed collectable biowaste as a carrier of polyacrylamide using a promising grafting method, in which the produced composite was a solid mass, not a hydrogel, which can be used as an effective heavy metal adsorbent. Lead was used due to its high toxicity. We assessed a number of parameters of grafted banana fibers before and after the adsorption. Additionally, we performed a kinetic study, in which we evaluated different adsorption conditions.

Experimental

Materials

Samples of banana pseudo-stems without any disease symptoms were collected from a private farm in Giza Governorate, Egypt. Acrylamide (Am) was purchased from Alpha Chemika (Mumbai, India). *N*,*N*'-methylenebisacrylamide (MBAm) was bought from Acros Organic NV (Geel, Belgium). Epichlorohydrin and lead nitrate were also manufactured by Alpha Chemika. All chemicals and reagents were of analytical grade and ready to use.

Methods

Extraction of Banana Fibers

Leaf sheaths were stripped from banana pseudo-stems, and the fiber bundles were manually separated using a knife. Then, the outer part was held firmly and pulled out, followed thorough washing and drying of the obtained fibers.

Preparation of GCFP Films

Free-radical grafting was applied in a typical run; 0.5 g of banana fibers was dispersed in 100 m*l* of distilled water, followed by the addition of 0.1, 0.5, or 1.0 g Am, respectively, to examine the monomer concentration effect. The reaction mixture was next subjected to vigorous stirring for 1 h, followed by heating at 50 °C and the addition of MBAm. Then, 0.05 m*l* of epichlorohydrin was added dropwise. The grafted cellulose was collected after 5 h and washed with a double amount of ethanol and ether for the removal of excessive water. Finally, the grafted fibers were dried in Petri dishes overnight at 50 °C.

Characterization of Films

Characterizations of the prepared GCFP films were carried out via ATR-FTIR spectroscopy (Spectrum Two IR Spectrometer - PerkinElmer, Inc., Shelton, CT, USA). All spectra were obtained by 32 scans and 4 cm^{-1} resolution in wavenumbers ranging from 4000 to 400 cm^{-1}. Scanning electron microscopy with energy dispersive electron spectroscopy (SEM-EDX) was employed for assessment of the non-destructive energy dispersive X-ray (EDX) unit attached to a scanning electron microscope (JSM 6360 L V, JEOL/Noran; JEOL, São Paulo, Brazil). Surface morphology imaging of different samples was recorded using an accelerating voltage of 10-15 kV.

Adsorption of Lead

A flame atomic absorption spectrometer (Agilent Technologies 200 Series AA; Santa Clara, CA, USA) was used for lead concentration determination. A pH meter (Hanna Instruments Inc., Woonsocket, Rhode Island, USA) was utilized for pH adjustment.

The adsorption experiments were performed in a set of 50-m*l* glass vials containing different masses of GCFP films and 20 m*l* of Pb aqueous solutions with an initial concentration (C_i). The mixture within the vial was subjected to shaking, and 1 m*l* was withdrawn at predetermined time intervals for analysis with the flame atomic absorption spectrometer (C_t). The pH value was maintained within the desirable range using 0.1 M of HCl or NaOH. The percentage of Pb removal (R%) was calculated using the following equation:

$$R\% = \left(\frac{C_i - C_t}{C_i}\right) \times 100 \quad (1)$$

The amount of Pb uptake (q) within the adsorbent was calculated by the formula

$$q = (C_i - C_t) \times \left(\frac{V}{M}\right) \quad (2)$$

where V is volume of the solution (l) and M is mass of the added sorbent (g).

All tests were performed in triplicate under equal conditions, and the average values were recorded to minimize the experimental errors.

Kinetic Parameters of the GCFP Film

To determine the mechanism of the adsorption of Pb onto the GCFP film, pseudo-first- and pseudo-second-order models, as well as intraparticle diffusion kinetic models, developed based on the characteristics of the adsorbent were previously proposed [35].

Lagergren [36] suggested a linear pseudo-first-order kinetic model, described below. The integrated form of the model is

$$\log(q_{eq}-q_t) = \log q_{eq} - \frac{k_1}{2.303}t \tag{3}$$

where q_t is the amount of Pb adsorbed at time t (min), q_{eq} is the amount of Pb adsorbed at equilibrium, and k_1 is the rate constant of pseudo-first order adsorption.

The adsorption kinetics can also be given by a linear pseudo-second-order reaction [37]. The integrated linear form of this model is as follows:

$$\frac{t}{q_t} = \frac{1}{k_2 q_{eq}^2} + \frac{1}{q_{eq}}t \tag{4}$$

where k_2 is the pseudo-second order rate constant of Pb adsorption. The plot of t/q_t versus t of equation (4) gives a linear relationship, from which q_{eq} and k_2 can be determined from the slope and intercept of the plot, respectively if the second-order kinetic equation is applicable.

The non-linear pseudo-first-order kinetic model [36] expresses the mechanism of removal as an adsorption preceded by diffusion through a boundary. The non-linear form of the model is given in equation (5).

$$q_t = q_e(1-e^{-k_1 t}) \tag{5}$$

where q_e and q_t are the amount of lead adsorbed (mg/g) at equilibrium, at time t (min), respectively, and k_1 (min^{-1}) is the pseudo-first-order rate constant. The pseudo-first-order equation assumes the adsorption of one adsorbate molecule onto one active site on the adsorbent surface.

The non-linear pseudo-second-order kinetic model, first proposed by Blanchard *et al.* [38], is based on the assumption that adsorption follows a second-rate kinetic mechanism. The model depicts the sorption process as controlled by chemisorption comprising sharing or exchanging of electrons between the solute and the sorbent. It assumes the adsorption of one adsorbate molecule onto two active sites on the sorbent surface. It can be represented in the following form:

$$q_t = \frac{k_2 q_e^2 t}{1+k_2 q_e t} \tag{6}$$

where q_e and q_t are the amounts of lead adsorbed (mg/g) at equilibrium, at time t (min), respectively, and k_2 (g/mg/min) is the pseudo-second-order rate constant.

Intraparticle Diffusion Model

Since the aforementioned models cannot identify a diffusion mechanism, the intraparticle diffusion model has also been tested to find the rate controlling step. This model refers to the theory proposed by Weber and Morris [39]. In the model, the rate of intraparticle diffusion is a function of $t^{1/2}$, defined below and calculated by linearization of the given curve:

$$q_t = K_i t^{1/2} \tag{7}$$

where K_i is the intraparticle diffusion rate.

Equilibrium Parameters of the GCFP Film

Analysis of equilibrium of adsorption provides information about the capacity of the adsorbent. Adsorption isotherm is characterized by certain constant values which express the surface properties and affinity of the adsorbent. This type of adsorption isotherm is generally fitted to the Langmuir, Freundlich, or Dubinin-Radushkevich isotherm models at a given constant temperature [40].

Langmuir Model

The Langmuir model is valid for monolayer adsorption onto a surface with a finite number of identical sites which are homogeneously distributed over the adsorbent surface. The well-known expression of the Langmuir model is given as

$$\frac{C_{eq}}{q_{eq}} = \frac{1}{K q_{\max}} + \frac{C_{eq}}{q_{\max}} \tag{8}$$

where q_{eq} is the amount of Pb adsorbed on the adsorbent at equilibrium, C_{eq} is the equilibrium concentration in the solution, $q_{\max}$ is the maximum adsorption capacity and K is the adsorption equilibrium constant. A plot of C_{eq}/q_{eq} versus C_{eq} indicates a straight line of slope $1/q_{\max}$ and an intercept of $1/Kq_{\max}$.

Freundlich Model

The Freundlich model is an empirical equation based on adsorption on a heterogeneous surface suggesting that the binding sites are not equivalent and/or independent. Freundlich equation is expressed as

$$\ln q_{eq} = \ln K_F + \frac{1}{n}\ln C_{eq} \tag{9}$$

where K_F is an indicator of the adsorption capacity, and n is the adsorption intensity, respectively. From the plot of $\ln q_{eq}$ versus $\ln C_{eq}$, K_F and $1/n$, values can be obtained.

Dubinin-Radushkevich Model

The Dubinin-Radushkevich isotherm [41] is commonly used to estimate the mechanism of adsorption and assess the porosity properties of the adsorbent in addition to adsorption apparent energy. The direct equation of the D-R isotherm is estimated by equation (10) as follows:

$$\ln q_{eq} = \ln q_{\max} - K_{ads}\varepsilon^2 \tag{10}$$

$$\varepsilon = RT\ln\left(1+\frac{1}{C_{eq}}\right) \tag{11}$$

where R and T are the universal gas constant (8.314 J/mol/K) and absolute temperature (K), respectively. K_{ads} is Dubinin-Radushkevich isotherm constant (mol^2/kJ^2) and ε is Polanyi potential. By plotting $\ln q_{eq}$ versus ε^2, a straight line was formed with a slope equal to K_{ads} and intercept equal to $\ln q_{eq}$.

The Reusability Study

The reusability study was carried out via desorption of metal ions from GCFP using 0.5 N HCl. The strips were soaked in HCl solution for 5 min and washed with distilled water for 5 min. These processes were repeated four times. The strips were subjected to stirring at 500 rpm with distilled water for 1 h then dried in an oven at 70 °C and used. This process was repeated in each of the four reusability cycles.

Results and Discussion

Preparation of GCFP Films

Scheme 1 illustrates the process of cellulosic fibers production using the pseudo-stems of banana plants. The formation of films was carried out via free-radical grafting process of acrylamide (Am) in a presence of excessive water to induce the production of films not a hydrogel as described in Experimental section. Three different ratios of Am were prepared. The sample containing 0.5/0.5 g of fibers and Am was completed in the form of strips that were coherent and easy to be used. The produced films were used after dialysis.

Characterization of the Sorbent

The FT-IR spectra of pure cellulose banana fibers as well as polyacrylamide-grafted cellulose banana fibers after and before lead adsorption are depicted in Figure 1. The FTIR spectrum of pure banana fiber represents a traditional lignocellulosic fiber's spectrum. The peaks of the OH stretching vibration, C-H stretching, aromatic skeleton vibrations of lignin rings, and β-glycosidic linkage were assigned at 3304, 2900, 1611, and 1010 cm^{-1}, respectively [29,30]. The acrylamide-grafted banana fibers showed significant changes in the original FTIR peaks. The OH peak position appeared sharper as well as it had a small peak at

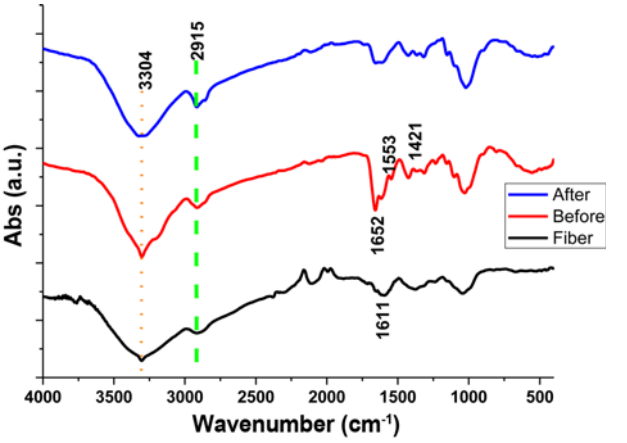

Figure 1. FTIR of original banana fibers and grafted banana fibers before and after Pb ions adsorption.

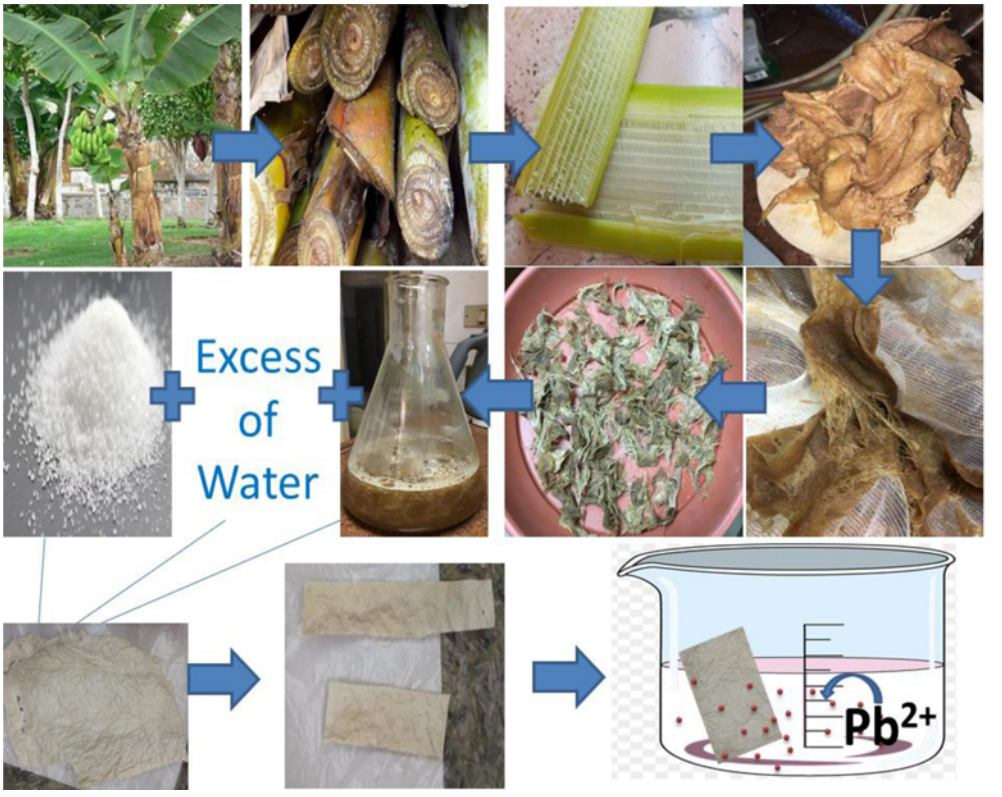

Scheme 1. Illustrated summary of the banana fiber processing as well as films formation and adsorption technique.

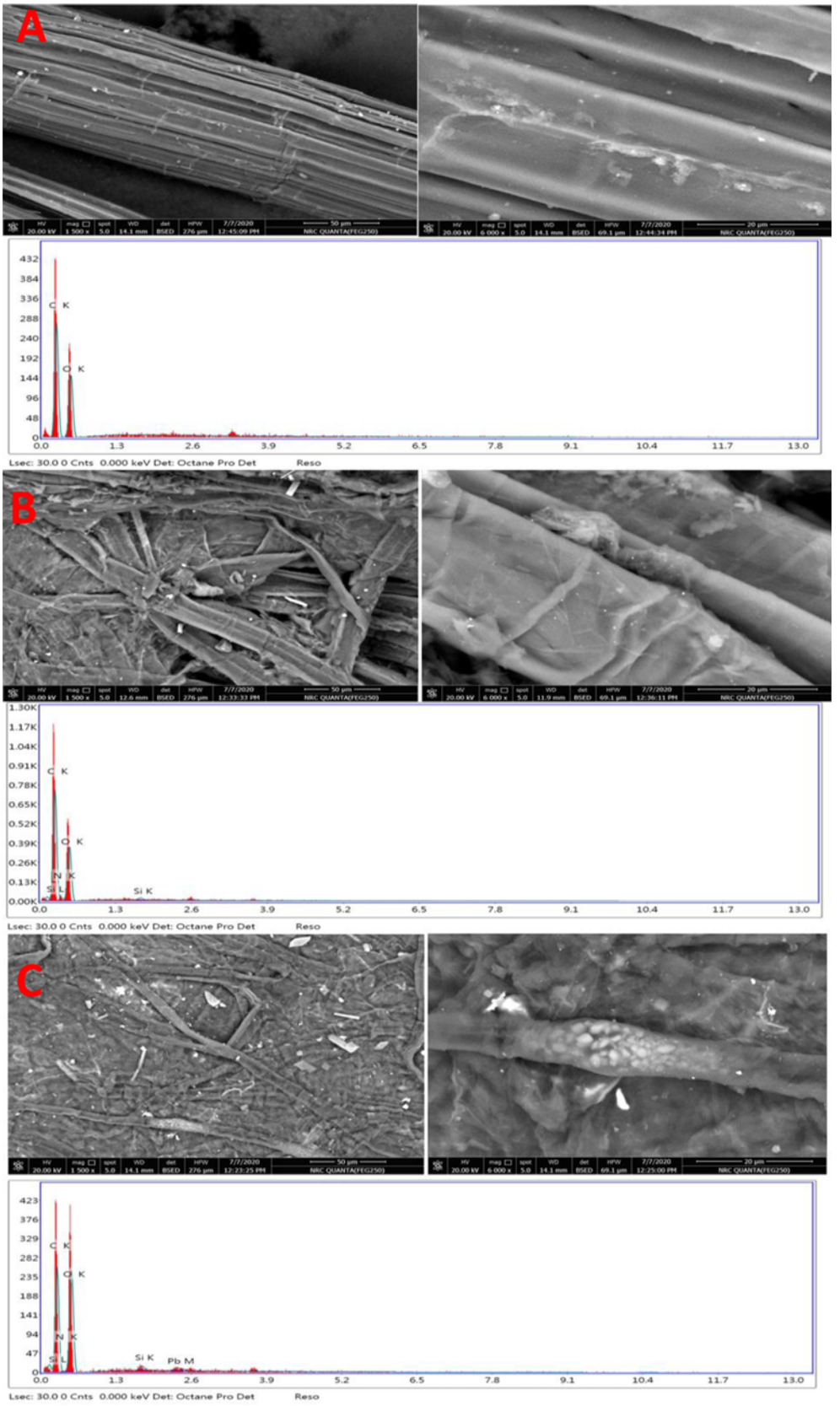

Figure 2. Topographical study and EDX of original banana fibers (A) and grafted banana fibers before (B) and after Pb ions adsorption (C).

around 3200 cm^{-1}, which referred to overlapping of O-H and N-H [42]. Additionally, the peak at 1652 cm^{-1} was characteristic for the C=O of the amide group. Grafting shifted the bands around 2900 cm^{-1} for C-H stretching vibrations to high frequency. The C-N band appeared at 1421 cm^{-1} as well as the peak of an ether linkage R-O-CH_2 which was formed by grafting appeared at 1115 cm^{-1} [42]. On the other hand, the adsorption of Pb ion affected the grafted banana fibers spectrum, and the peak at 3304 cm^{-1} appeared broad. The C-H stretching peak was split. Moreover, the bands at 1600 cm^{-1} area were with almost disappearing sharpness. In addition, the peak at 1652 cm^{-1} disappeared, which might have been due to the reaction that occurred and the attraction of a lead ion inside the film as well as to the overall the film surface. These resulted in a withdrawal of an electron of the amide group toward Pb, forming a new bond [43-46]. Hence, all changes in the FT-IR spectrum of the grafted banana fibers after the adsorption were responsible for Pb binding [47].

The adsorption of metals via a fibrous matrix can be investigated clearly and informatively with SEM topographical imaging. Figure 2 illustrates the SEM and EDX of the original cellulose banana fibers and the polyacrylamide-grafted cellulose banana fibers before and after the lead adsorption. Figure 2A presents the appearance and the texture of the original cellulose banana fibers, and the EDX chart which presented the fiber composition of C, O, and some trace elements found naturally in natural fibers. Figure 2B represents polyacrylamide-grafted cellulose banana fibers before Pb adsorption, where a thin layer-coated fibers with some wrinkles on the surface. The EDX chart visualizes the presence of a nitrogen atom as a result from grafting. Additionally, Figure 2C illustrates the SEM and EDX of polyacrylamide-grafted cellulose banana fibers after adsorption. The EDX chart contains a band for Pb. A metal particle referring to Pb is present in the SEM image. A high-magnification photo revealed that Pb was inserted into the fibers by adsorption. These results confirmed that the grafted fibers prepared in this study are a strong adsorbent for Pb ions.

Sorption Study

The effect of different operating conditions on the removal rate of Pb ions using GCFP film is presented in Figure 3.

Effect of the Contact Time

The effect of contact time on the removal rate of Pb ions by the GCFP film is depicted in Figure 3A. An experiment was performed in the time range 5-120 min at pH 7, 50 ppm of Pb, and an adsorbent dose of 0.4 g. From the figure, it is clear that the removal of Pb increased sharply within the first 30 min (90 %), and then slowly reached the equilibrium point at 60 min (98 %). This outcome was due to the vacant status of the adsorption sites on the GCFP film during the initial stage; hence, Pb (II) ions bound to them. Gradually, with increase in the contact time duration, the number of active adsorption sites decreased, which affected the further

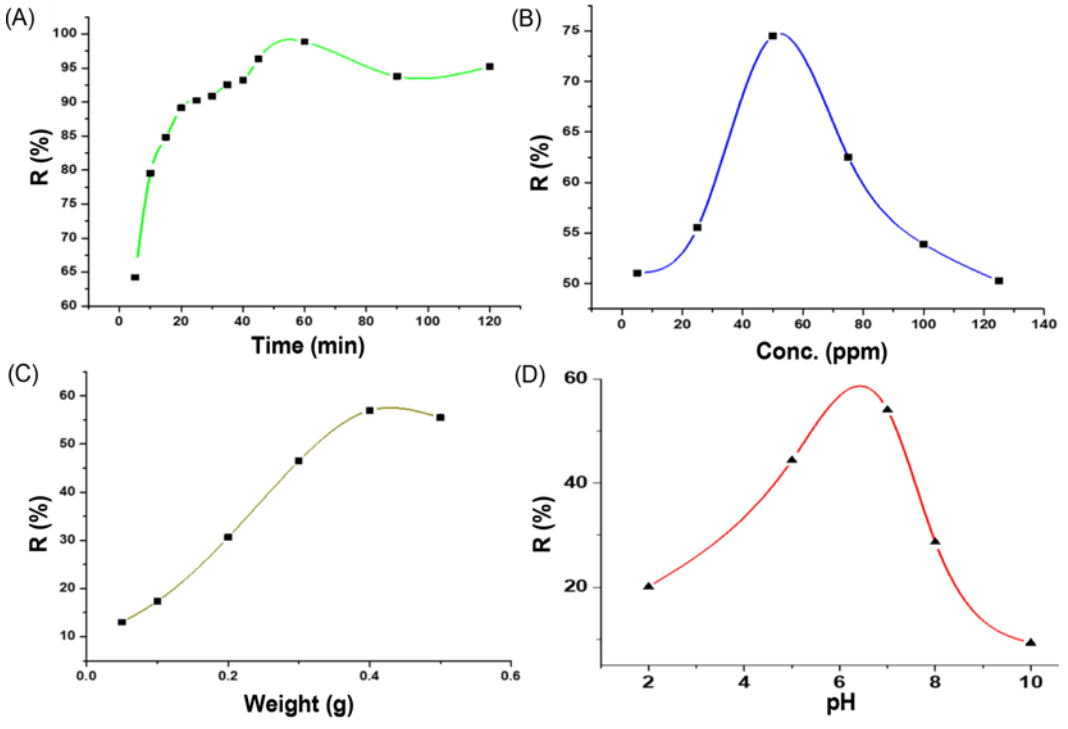

Figure 3. Effect of different operating conditions on the Pb removal rate; (A) effect of the contact time, (B) effect of the initial concentration, (C) effect of the adsorbent dose, and (D) effect of pH.

adsorption of Pb ions [48].

Effect of the Initial Concentration

Figure 3B illustrates the influence of initial Pb ion concentrations on the removal rate within a concentration range from 5 ppm to 125 ppm and pH 7 in 20 m*l* of Pb solution and an adsorbent dose of 0.4 g in a time period of 30 min. It is evident from the figure that the removal rate (*R*%) increased with rise in the initial Pb concentration to 50 ppm, at which this rate reached 74 % but then slowly decreased to 125 ppm. This effect was due to the relatively higher number of the existing binding sites of the adsorbent and low Pb concentrations. Hence, higher *R*% was reached, whereas, at high Pb concentrations, the binding sites were saturated and could not adsorb more Pb ions, leading to a lower *R*% [49].

Effect of the Adsorbent Dose

Figure 3C shows the removal of Pb by the GCFP film at different weights (0.05, 0.1, 0.2, 0.3, 0.4, and 0.5 g). The experiment was carried out using 20 m*l* of 50 ppm of Pb solution at pH 7 for 30 min. It is visible from the figure that the increase in the adsorbent weight augmented the removal rate; it's the maximum value of the removal rate rose from 13 % to 56 % along the increase in the weight from 0.05 to 0.4 g. This outcome may be attributed to the presence of a large number of adsorption sites and/or the existence of a greater surface area, which promoted the adsorption [50].

Effect of pH

Figure 3D shows the effect of solution pH on the removal

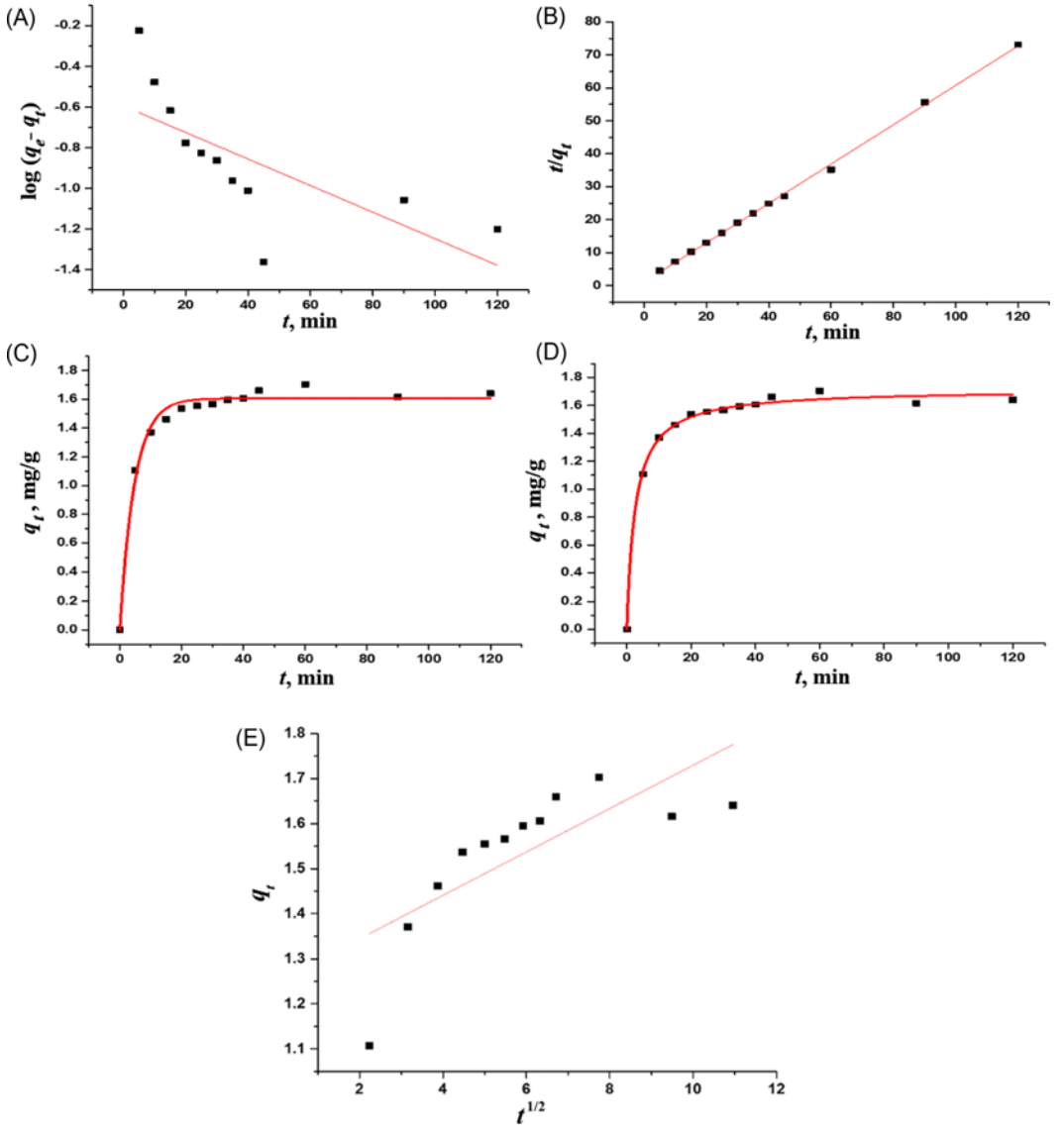

Figure 4. Different adsorption kinetics of Pb on (on or with) cellulosic fiber/polyacrylamide film; (A) linear pseudo-first order model, (B) linear pseudo-second order model, (C) non-linear pseudo-first order model, (D) non-linear pseudo-second order model, and (E) intraparticle diffusion model.

rate of Pb ions by the GCFP film, which changed in the range from 2 to 10. This experiment was performed within 30 min at a Pb concentration of 50 ppm and an adsorbent dose of 0.2 g. Obviously, the increase in the pH of the acidic medium elevated the removal rate until neutral pH was reached, and then it decreased under alkaline conditions of the medium. This process occurred due to the negative effect of the alkaline media on the functional groups of the adsorbent, which were blocked and deactivated by sodium ions. In contrast, in acidic media the functional groups were free and active.

Kinetic Parameters of the Adsorption

In this study, five models were applied to investigate the kinetics of Pb adsorption on the GCFP film: linear and non-linear pseudo-first- and pseudo-second-order models, as well as an intraparticle diffusion model. The linearized and non-linearized plots of the models as well as intraparticle diffusion are represented in Figure 4. The values of the constants k_1, k_2, $q_{eq,cal}$, and the correlation coefficients are listed in Table 1. Generally, the R^2 value was employed to decide the suitability of the model for adsorption kinetics description [51-53]. Meanwhile, the other values were consequently followed. In the linear models, R^2 values for the pseudo-first- and the pseudo-second-order were 0.5014 and 0.9789, respectively.

Otherwise, the non-linear pseudo-first- and pseudo-second-order models were determined to elucidate the kinetics of Pb adsorption. The R^2 value of the non-linear pseudo-first-order model was 0.8312, which is considerably lower than the R^2 of the linear pseudo-second-order model. Similarly, the R^2 of the non-linear pseudo-second-order model was 0.9557, which was also lower than the R^2 of the linear pseudo-second-order model. Finally, the results obtained in the kinetics study confirmed that the linear pseudo-second-order model is the optimal model that could describe the adsorption kinetics of Pb adsorption on GCFP film. Therefore, based on the abovementioned our results, it could be concluded that the linear pseudo-second-order model describes the best adsorption mechanism of Pb on GCFP film with a k_2 value of 0.3927 and $q_{eq,cal}$=138.78 mg g^{-1}, which was in close proximity to the actual one.

On the other hand, the mechanism of Pb adsorption by GCFP film can be elucidated using the Weber and Morris intraparticle diffusion model. According to this model, adsorption occurs in three consecutive steps: external diffusion, intraparticle diffusion, and adsorption, each of which can affect the adsorption process. From Figure 4E, we can suggest that the first linear stage is a rapid external diffusion, where surface adsorption is negligible, the second is an adsorption stage, in which intraparticle diffusion is limited, and the final stage is the stage of equilibrium. Because the linear plot does not pass through the origin, the intraparticle diffusion is not just a controlling step. As seen in the figure, the diffusion rate, K_i=0.0481, and the correlation coefficient (R^2) is 0.5699.

Determination of the Equilibrium Parameters

Langmuir, Freundlich, and Dubinin-Radushkevich isotherms are the most widely used models for description of adsorption systems. Determination of the equilibrium isotherms in both of them was conducted at different initial Pb concentrations, from 5 to 125 ppm. Figure 5A, B represents the different forms of the isotherm plots and the correlation coefficients as well as isotherm constants are also listed in Table 2. As can be seen in Table 2, a lower R^2 value was observed in the Langmuir model than in the other studied models as well as so far q_{max} than the practical one. Additionally, the Freundlich model represents a more acceptable R^2 value than that of the Langmuir model. However, the Dubinin-Radushkevich model had better fitting of the adsorption data, based on its R^2 value of 0.9972, which was the highest of all models; the Dubinin-Radushkevich model q_{max} was also in agreement with the actual q_{max}. The Dubinin-Radushkevich model is based on the adsorption on a heterogeneous surface, suggesting differences in the binding sites, which were not equivalent and/or independent. Thus, the surface of the GCFP film was expected to have nonhomogeneous active sites for adsorption, and a much better fit was obtained.

Reusability

The reusability of GCFP film was used in four cycles of adsorption (Table 3). As stated previously, the first cycle of adsorption was recorded to be 128 mg of Pb/g of GCFP film. The reusability of the GCFP film was determined through the decrease in the adsorption activity after the first cycle, where the adsorption capacity of the film decreased by approximately 20 %. The third and fourth cycles were characterized by an approximate decrease to 50 % of the capacity. These results affirmed the strong attraction of the GCFP film to Pb leading to its adsorption from the solution, which filled the pores and the active surface sites of the GCFP film [17]. The washing process removed only

Table 1. Pseudo-first- and second-order reaction rate parameters for linear and non-linear fitting

Linear fitting						Non-linear fitting					
First order kinetic model			Second order kinetic model			First order kinetic model			Second order kinetic model		
k_1	$q_{eq,cal}$ (mg/g)	R^2	k_2	$q_{eq,cal}$ (mg/g)	R^2	k_1	$q_{eq,cal}$ (mg/g)	R^2	k_2	$q_{eq,cal}$ (mg/g)	R^2
0.01497	3.93	0.5014	0.3927	138.78	0.9789	0.208	1.606	0.8312	0.223	1.715	0.9557

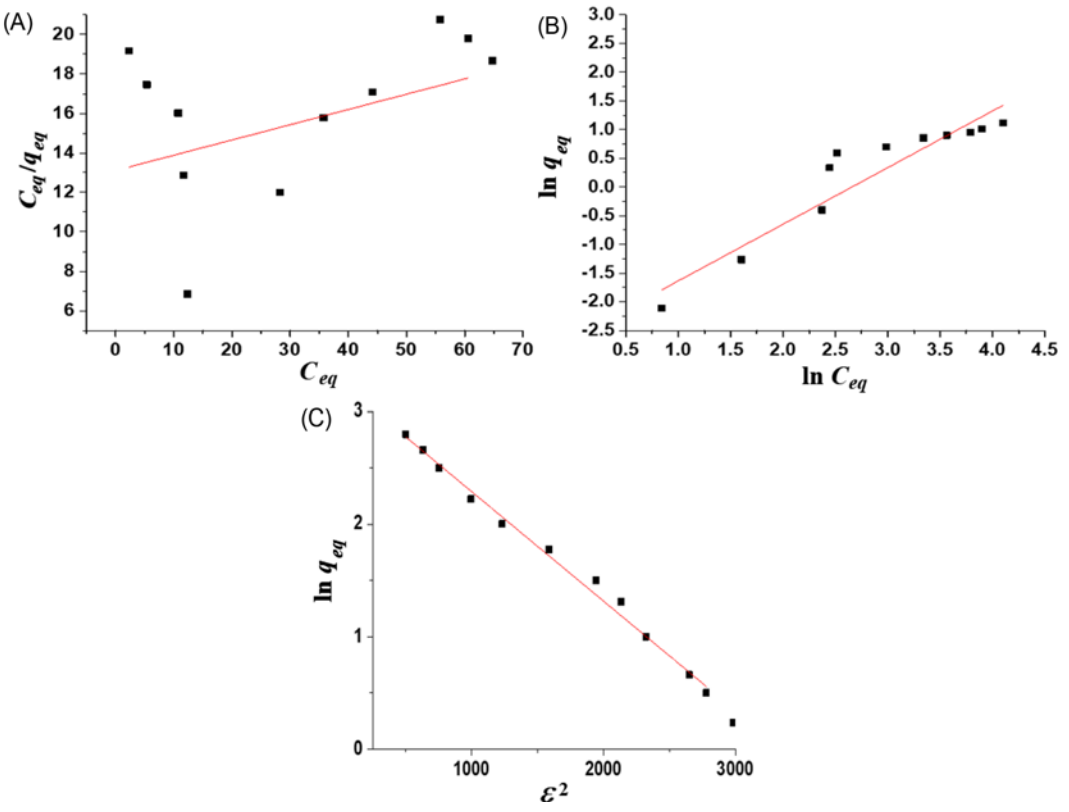

Figure 5. Linearized Langmuir and Freundlich adsorption isotherms of Pb ions on cellulosic fiber/polyacrylamide film; (A) Langmuir model, (B) Freundlich and Dubinin-Radushkevich models, and (C) isotherm model.

Table 2. Isotherm constants for the adsorption of Pb on the GCFP film

Langmuir isotherm			Freundlich isotherm			Dubinin-Radushkevich isotherm		
q_{max} (mg/g)	K (mg/g)	R^2	K_F	n	R^2	q_{max} (mg/g)	K_{ads} (mol^2/kJ^2)	R^2
13.33	0.0057	0.3879	0.076	1.015	0.9147	132	0.000433	0.9982

Table 3. Adsorption amounts of Pb ions on the GCFP film in four adsorption-desorption cycles

Cycle number	Amounts of lead adsorbed (mg/g)
1	128
2	100
3	50
4	48

approximately 70 % of the absorbed Pb ions, while the remaining percentage was attached strongly to the GCFP film. This shows that the GCFP film is a strong chelator of Pb ions in aqueous solutions [18].

Conclusion

In the present study, we examined the application of biowaste materials for the removal of a hazardous water contaminant, the heavy metal Pb. We produced solid film strips based on polyacrylamide-doped banana tree-extracted cellulosic fiber, which were effective and easily usable and recyclable. The efficiency of lead ions adsorption was investigated by varying the operating conditions. We also examined the kinetics and equilibrium aspects of the process. Our results showed that the adsorption efficiency was considerably affected by the operating conditions. The highest adsorption efficiency of 98 % was achieved at pH=7, an adsorbent dose of 0.4 g, initial Pb concentration of 50 ppm, and a contact time duration of 60 min. The results of the kinetics assessment revealed that the pseudo-second-order model was a better fit of the adsorption data. Intraparticle diffusion can effectively be used as one of the controlling steps. An equilibrium study was carried out by applying the Langmuir, Freundlich, and Dubinin-Radushkevich isotherm adsorption models. We found that the Dubinin-Radushkevich isotherm adsorption model represented the

best fitting model. The strips used here for Pb ions removal from water were produced from inexpensive and environmentally clean materials (biowaste). Additionally, our reusability study confirmed the strong chelating ability of the GCFP film toward Pb ions. Our GCFP film has good reusability, whose efficiency, however, declines after the reuse second cycle.

Acknowledgment

We would like to express our deep appreciation and sincere gratitude to the National Research Centre in Cairo, Egypt, for the financial support of this study. Cordial thanks are also due to Hainan Key Laboratory of Banana Genetic Improvement, Haikou Experimental Station, the Chinese Academy of Tropical Agricultural Sciences (Haikou, Hainan, China) for their real valuable support during the conducting of this study and the preparation of the present manuscript.

References

1. M. S. Hasanin, *Environ. Sci. Pollut. Res.*, **27**, 26742 (2020).
2. Q. Lin, M. Gao, J. Chang, and H. Ma, *Carbohydr. Polym.*, **151**, 283 (2016).
3. A. Gürses, M. Yalçin, and C. Dogar, *Water Air Soil Pollut.*, **146**, 297 (2003).
4. V. P. Kasperchik, A. L. Yaskevich, and A. V. Bil'Dyukevich, *Pet. Chem*., **52**, 545 (2012).
5. J. Mao, S. W. Won, J. Min, and Y.-S. Yun, *Korean J. Chem. Eng.*, **25**, 1060 (2008).
6. N. Hidalgo, G. Mangiameli, T. Manzano, G. G. Zhadan, J. F. Kennedy, V. L. Shnyrov, and M. G. Roig, *Biotechnol. Bioprocess Eng.*, **16**, 821 (2011).
7. A. R. Rahmani, K. Godini, D. Nematollahi, G. Azarian, and S. Maleki, *Korean J. Chem. Eng.*, **33**, 532 (2016).
8. R. K. Gautam, A. Mudhoo, G. Lofrano, and M. C. Chattopadhyaya, *J. Environ. Chem. Eng.*, **2**, 239 (2014).
9. M. Martín-Lara, G. Blázquez, A. Ronda, I. Rodríguez, and M. Calero, *J. Ind. Eng. Chem.*, **18**, 1006 (2012).
10. S. S. Subhashini, M. Velan, and S. Kaliappan, *J. Environ. Biol.*, **34**, 831 (2013).
11. W. Wei, X. Liu, P. Sun, X. Wang, H. Zhu, M. Hong, Z.-W. Mao, and J. Zhao, *Environ. Sci. Technol.*, **48**, 3363 (2014).
12. L. Järup, *Br. Med. Bull.*, **68**, 167 (2003).
13. M. Jaishankar, B. B. Mathew, M. S. Shah, and K. R. S. Gowda, *J. Environ. Pollut. Hum. Health*, **2**, 1 (2014).
14. P. C. Nagajyoti, K. D. Lee, and T. Sreekanth, *Environ. Chem. Lett.*, **8**, 199 (2010).
15. M. Lambert, B. A. Leven, and R. M. Green, "New Methods of Cleaning Up Heavy Metal in Soils and Water", Environmental Science and Technology Briefs for Citizens, Kansas State University, Manhattan, KS, 2000.
16. F. Wang, Y. Pan, P. Cai, T. Guo, and H. Xiao, *Bioresour. Technol.*, **241**, 482 (2017).
17. W. Shen, S. Chen, S. Shi, X. Li, X. Zhang, W. Hu, and H. Wang, *Carbohydr. Res.*, **75**, 110 (2009).
18. X. Jin, Z. Xiang, Q. Liu, Y. Chen, and F. Lu, *Bioresour. Technol.*, **244**, 844 (2017).
19. S. Flora, M. Mittal, and A. Mehta, *Indian J. Med. Res.*, **128**, 501 (2008).
20. A. Evens, D. Hryhorczuk, B. P. Lanphear, K. M. Rankin, D. A. Lewis, L. Forst, and D. Rosenberg, *J. Environ. Health*, **14**, 21 (2015).
21. M. Dikilitas, S. Karakas, and P. Ahmad, "Plant Metal Interaction", p.41, Elsevier, 2016.
22. A. R. Cohen, M. S. Trotzky, and D. Pincus, *J. Pediatr.*, **67**, 904 (1981).
23. M. Jurdziak, P. Gać, H. Martynowicz, and R. Poręba, *Environ. Toxicol. Pharmacol*., **39**, 1034 (2015).
24. M. Abdelraof, S. Ibrahim, M. A. Selim, and M. Hasanin, *J. Environ. Chem. Eng.*, **8**, 103870 (2020).
25. M. S. Hasanin, O. M. Darwesh, I. A. Matter, and H. El-Saied, *Biocatal. Agric. Biotechnol.*, **17**, 160 (2019).
26. M. S. Hasanin, A. H. Hashem, E. S. Abd El-Sayed, and H. El-Saied, *Cellulose*, **27**, 4443 (2020).
27. A. H. Hashem, M. S. Hasanin, A. M. A. Khalil, and W. B. Suleiman, *Waste Biomass Valori.*, **11**, 5721 (2020).
28. S. Ibrahim, H. Elsayed, and M. Hasnein, *J. Polym. Environ.*, **29**, 472 (2021).
29. A. Youssef, M. Hasanin, M. Abd El-Aziz, and O. Darwesh, *Heliyon*, **5**, e01332 (2019).
30. M. Abdelraof, M. S. Hasanin, and H. El-Saied, *Carbohydr. Polym.*, **211**, 75 (2019).
31. H. El-Saied, A. H. Basta, M. E. Hassanen, H. Korte, and A. Helal, *J. Polym. Environ.*, **20**, 838 (2012).
32. U. N. E. P. Dtie, Compendium of Technologies, Osaka, United Nations Environment Programme, 2009.
33. M. Mostafa and N. Uddin, *Case Stud. Constr. Mater.*, **5**, 53 (2016).
34. S. S. Bagali, B. S. Gowrishankar, and A. S. Roy, *Engineering*, **3**, 409 (2017).
35. L. Zheng, Z. Dang, X. Yi, and H. Zhang, *J. Hazard. Mater.*, **176**, 650 (2010).
36. S. Lagergren, *Handlingar*, **24**, 1 (1898).
37. H. Ys, G. Mckay, H. Ys, and G. Mckay, *Process Biochem.*, **34**, 451 (1999).
38. G. Blanchard, M. Maunaye, and G. Martin, *Water Res.*, **18**, 1501 (1984).
39. W. Weber and J. Morris, "Proceedings of the First International Conference on Water Pollution Research", p.231, 1962.
40. I. Langmuir, *J. Am. Chem. Soc.*, **38**, 2221 (1916).
41. A. E. Abdelhamid, A. Labena, E. S. Mansor, S. Husien, and R. M. Moghazy, *Biomass Conv. Bioref.*, https://doi.org/10.1007/s13399-020-01250-7 (2021).
42. S. Dacrory, H. Abou-Yousef, R. E. Abouzeid, S. Kamel, M. S. Abdel-aziz, and M. El-badry, *Int. J. Biol. Macromol.*,

117, 179 (2018).
43. K. Stana-Kleinschek, S. Strnad, and V. Ribitsch, *Polym. Eng. Sci.*, **39**, 1412 (1999).
44. B. Siffert and J.-M. Metzger, *J. Colloids Surf.*, **53**, 79 (1991).
45. Y. Li, L. Cao, L. Li, and C. Yang, *J. Hazard. Mater.*, **289**, 140 (2015).
46. R. Kumar, R. K. Sharma, and A. P. Singh, *Sep. Purif. Technol.*, **219**, 249 (2019).
47. P. Chand and Y. B. Pakade, *J. Chem.*, **2013**, 164575 (2013).
48. S. Peng, H. Meng, Y. Ouyang, and J. Chang, *Ind. Eng. Chem. Res.*, **53**, 2106 (2014).
49. S. Cengiz and L. Cavas, *Bioresour. Technol.*, **99**, 2357 (2008).
50. M. A. Al-Ghouti, M. A. Khraisheh, M. N. Ahmad, and S. Allen, *J. Hazard. Mater.*, **165**, 589 (2009).
51. R. M. Abdelhameed, M. Taha, H. Abdel-Gawad, and B. Hegazi, *J. Mol. Liq.*, **327**, 114852 (2021).
52. H. E. Emam, H. B. Ahmed, and R. M. Abdelhameed, *Carbohydr. Polym.*, **266**, 118163 (2021).
53. H. E. Emam, M. El-Shahat, and R. M. Abdelhameed, *J. Hazard. Mater.*, **414**, 125509 (2021).